INDIAN JOURNAL OF
ENGINEERING

18(50), 2021

To Cite:
Messioud S, Mokhbi H, Khelalfa H, Khelalef, Ishaq Laouar. Collapse Investigation and Numerical analysis of the Repair and completion of the Twin-Tube Tunnel of Jebel El-Ouahch T1 in Constantine Province, Algeria. *Indian Journal of Engineering*, 2021, 18(50), 240-257

Author Affiliation:
[1]Civil Engineering and Environment Laboratory (LGCE), University of Jijel, Jijel, Algeria
[2]Department of Civil Engineering, University of 20 Aout Skikda, Skikda, Algeria
[3]Department of Civil Engineering, Faculty of Engineering and Technology, Selinus University of Science and Literature (SUSL), Bologna, Italy

✉**Corresponding author:**
E-mail: khelalfahoussam@gmail.com

Peer-Review History
Received: 27 May 2021
Reviewed & Revised: 29/May/2021 to 21/June/2021
Accepted: 23 June 2021
Published: June 2021

Peer-Review Model
External peer-review was done through double-blind method.

Collapse Investigation and Numerical analysis of the Repair and completion of the Twin-Tube Tunnel of Jebel El-Ouahch T1 in Constantine Province, Algeria

Salah MESSIOUD[1], Hicham MOKHBI[2], Houssam KHELALFA[1,3,✉], Mohammed KHELALEF[1], Ishaq LAOUAR[1]

ABSTRACT

A numerical analysis of the rehabilitation of the DJBEL ELOUAHCH tunnel at the East-West Motorway of Algeria, was carried out following a partial landslide of its left tube, using the PLAXIS 2D calculation code which is based on the finite element method (FEM). The goal is to design a model of this tunnel reinforced with fiberglass bolts and show the excavation influence of the left tube on the right tube during the repair phases; In order to establish a study on the behavior of the latter to enhance the solutions applied in this case. A simplified approach is used to strengthen the tunnel's forehead numerically and replace the bolts and soil / bolt interaction with an equivalent parameter (increase cohesion and friction angle of the soil). In this context, The Iraratna Model [1988, 1990] was used to determined the equivalent geotechnical characteristics of the tunnel to be repaired. During this study, the repair phasing of the old tube was taken into consideration phase by phase with an elasto-plastic behaviour law. To facilitate the calculation, in situ measurements were implemented to estimate the deconfinement at each calculation phase; the variation of vertical and horizontal displacements and the variation of the stresses are presented according to the phases of the tunnel rehabilitation works.

Keywords: Tunnel, Partial Landslide, Rehabilitation, Stresses, Displacements, homogenization, Numerical Modeling.

1. INTRODUCTION

Tunnel projects can be different in terms of their depths, geometries, lithology, excavation methods ...etc. [1]. Among the most difficult problems that must

be considered about tunnels are; the retention of the massive response surrounding the structure, determining the types and characteristics of the support to be implemented to ensure the strength of the walls (retaining calculation) and the estimation of displacements, deformations and stresses [2,3]. On the other hand in modern times, drilling techniques are improving with increasingly powerful machines, the use of more efficient explosives, the use of hangers and shields, the use of the tunnel boring machine and the treatment of difficult grounds by injections or freezing [4-15]. The digging of tunnels in soft ground generally requires reinforcement of the working forehead by pre-supporting or pre-confinement techniques in order to avoid possible landslides at the level of the tunnel forehead, the consequences of which can be catastrophic for the worksite personnel on the one hand, and to preserve the stability of the structure and minimize the deformation of the surrounding massif on the other hand [16-20]. The use of traditional excavation techniques must be complemented by measures to confine the forehead and implement as quickly as possible the provisional support. This can be achieved, at least partially, by the technique of pre-support which consists in setting up in the tunnel forehead, a peripheral support, either with the help of reinforcements forming an umbrella vault or by a pre-vault obtained by sawing a peripheral groove filled with sprayed concrete [21- 24].

The repair works are usually expensive, on the one hand because they require expensive techniques and products, on the other hand because they are often subject to significant constraints due to the need to maintain the structure in operation (partially or totally). Among the currently used methods include the method called "the fiberglass bolts" and the umbrella vault method. The FIT (FRP Injection Tube) method is a pre-confinement technique that consists of reinforcing the working face/ or tunnel forehead by bolting using tubular inclusions/ or injection tube in GFRP (glass fiber reinforced polymer) sealed in the ground by injection system using a cement grout in order to stabilize the tunnel forehead (Crown/ Calotte and Bench/ Stross) and to oppose the deformations and stresses generated by the ground movement in different directions [25- 33]. Controlling the stability of an underground structure during repair works is a particularly complex issue, the behavior of the rock mass in which the underground structure was dug (repair area) is often complex and difficult to predict [34- 37]. However, despite the effectiveness of the fiberglass bolt method actually recorded on site, the soil / bolt behavior is still difficult to apprehend given the heterogeneity of the soil / bolt environment [38, 39]. Currently with the development of science and technology, there are several tools for making a rigorous study of the structure being repaired, such as numerical computer codes; thus, auscultation devices which allow continuous and reliable monitoring of the structure's behavior [40- 51].

The fiberglass bolt reinforcement method was used with the umbrella vaults during repair works on the tunnel which suffered a partial landslide on January 2014 at Constantine province, in Algeria. The accident caused the condemnation of part of the left tunnel tube, which had served for three months only after provisional reception of the project. This paper will present the effects of the phases of carrying out the repair works on the behavior of the two left and right tubes, the repair phasing may be performed by a numerical model in finite elements FEM (PLAXIS 2D). The main objective of this study is to establish a two-dimensional numerical model which representing the actual behavior of the tunnel during the repair phases of the old tunnel which was destroyed after commissioning, and the reinforcement of the tunnel forehead by the fiberglass bolts method as well as the actual phasing of the digging were taken into consideration in the modeling. The homogenization method [52] was used for the determination of the numerical parameters of the 2D model.

2. GEOLOGY, HYDROGEOLOGY AND GEOTECHNICAL SURVEYS OF TUNNEL T1 AREA

The T1 tunnel is part of the East-West motorway, between the CONSTANTINE province and the SKIKDA province, the latter located to the North East of Constantine province. It crosses Djebel El Ouahch to the right of the natural park. Due to the project's coastlines and the need to maintain acceptable slopes and ramps along the motorway, the use of the tunnel is required (Figure 1a). And that is why Crossing the rugged terrain between kilometric points KP 205 + 393 and KP 207 + 284,5. In dimensional terms, the tunnel is a twin-tube approximately 1891m long, with a section in the form of a low vault about 190 m2. The maximum tunnel coverage was 140 m. The width of the excavation section is approximately 18m and the width of the central pillar is approximately 17m. The longitudinal slope of the tunnel being 4%. Interconnection galleries are designed there every 380 m approximately.

ISSN 2319–7757 EISSN 2319–7765 I OPEN ACCESS

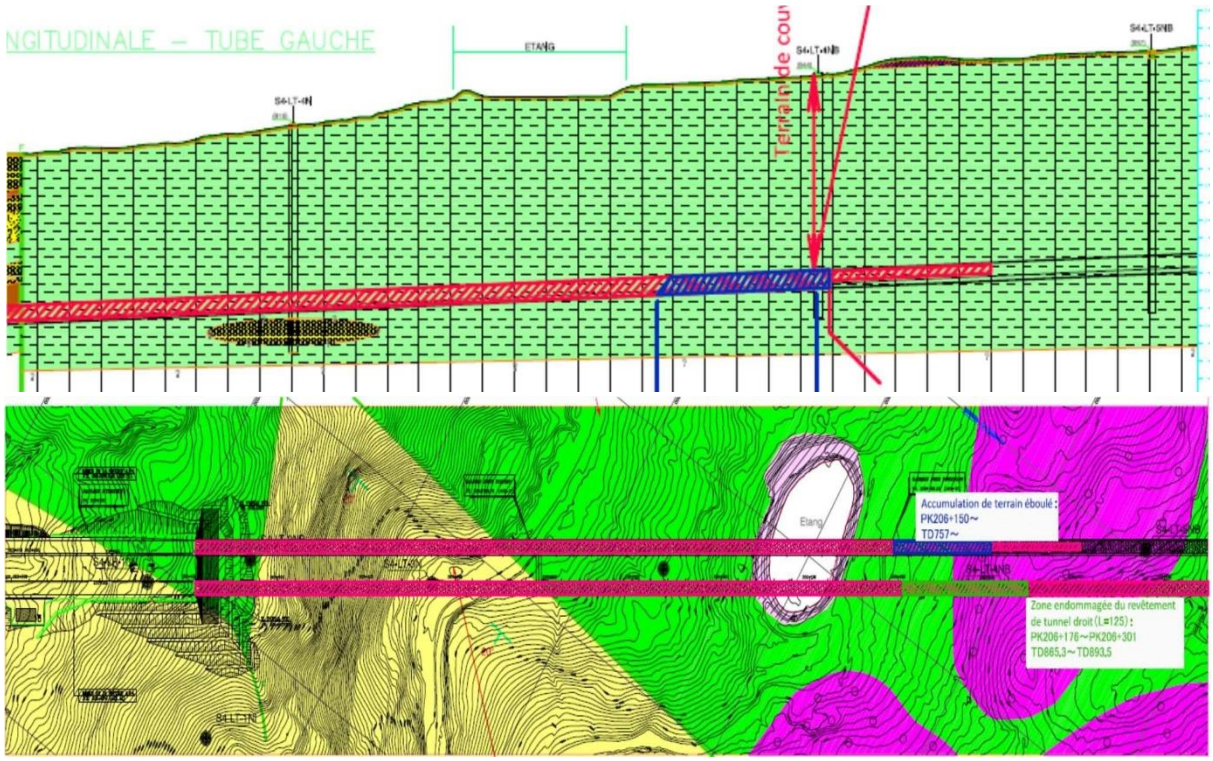

Figure 1: a) Geological model planned in the design phase for the collapse area.

From a geomorphological point of view, the T1 tunnel crosses the wooded mountainous area of DJebel El Ouahch (figure 1a). The geological map of El Aria at 1: 50,000 th shows a complex structure [53]. The large lithological groups are represented by thrust sheets dominated by marly and marly-limestone units at the base, of Cretaceous age. These units are covered, in the DJebel Ouahch region (figures 1b and 1c), by the Numidian (Oligocene) sheet formed by coarse sandstones, massive, at the top and clays at the base. Thick colluvium, several tens of meters, coarse, with sandstone blocks and a sandy matrix, of Quaternary age, largely cover the allochthonous formations [54, 55].

(b) (c)

Figure 1 : b) Colluvium with large sandstone blocks, Tunnel T1, KP 206 + 350, c) Numidian sandstone dislocated and covered with scree, at the level of the South Portal of the T1 tunnel.

Figure (2) shows the local geology of the tunnel in the intervention area, reconstructed in the design phase on the basis of geognostic and geophysical investigations carried out in 2011. The data collected in the intervention area include n.3 geognostic soundings (S4-LT-04N, S4-LT- 04NB, S4-LT-05NB) and n.3 two-dimensional tomographies reconstructed by the Vertical Electrical Soundings (VES) method. The electrical resistivity method was applied and implemented according to 3 parallel acquisition axes and these parallel to the line of the tunnel.

ISSN 2319–7757 EISSN 2319–7765 I OPEN ACCESS

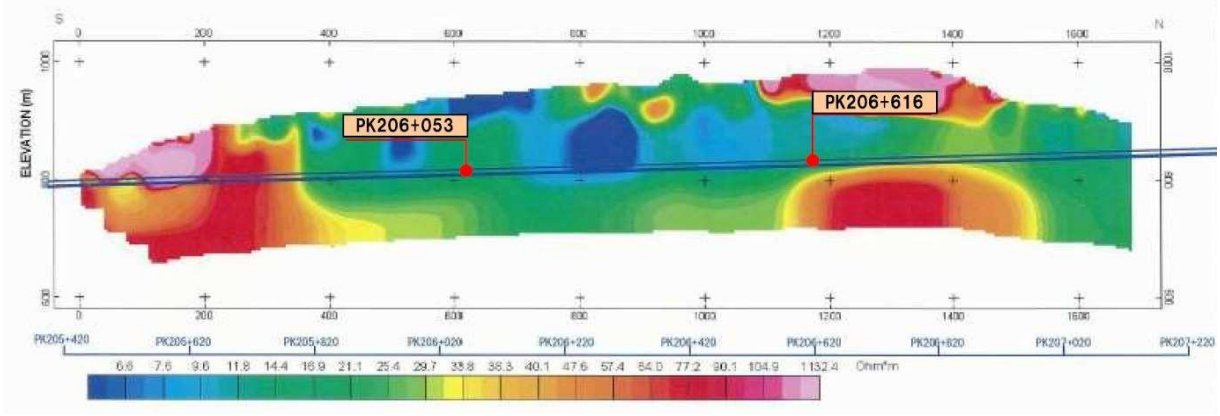

Figure 2 : Two-dimensional tomograms reconstructed by the (VES) method in the design phase.

Based on the geological model designed, it can be observed that in the intervention area:

- The tunnel is located entirely in the marly and marl-limestone formation corresponding to the Tellian nappe of Campanian – Maastrichtian age and in particular in the geological unit of the Cretaceous clay-stones.
- At the surface (Figures 1b and 1c), the lithological formation of Quaternary colluviums outcrops locally. Coarse colluvium is represented by heterometric sandstone elements: pebbles and angular blocks coated in a ruddy silty matrix.
- Beside the tunnel, geophysical surveys showed the presence of an area of low electrical resistivity extended, along the left tube, between KP 205 + 900 and KP 206 + 550 approximately.

Figure 3 : Shale rock in the middle of Tunnel T1.

Along the tunnel, the water level in drill hole LT-04 was measured at a depth of 91 meters, either within the horizon sandstone which is underlying the calystones/ shales (Figure 3). The sandstone horizon thus acts as a draining layer under the shales. While the LT-05NB drill holes revealed surface water. The clayey nature of the formations encountered could thus form a tight barrier to infiltrated water.

3. ACCIDENT EFFECTS DESCRIPTION

In order to investigate the extension of the decompression zone induced by the collapse, 22 vertical soundings were carried out at the tunnel depth. The material deformation state was investigated listing, logs and measuring the velocity of propagation of seismic waves. However, only the measurement of the perforation water losses allowed the definition of the decompressed zone, on the other hand it is not possible to define a correlation between the waves velocity (S) with the shale rock density. Only 8 boreholes between the 22nd conducted showed significant water loss and 7 were on the axis of the left tube. The Curve would appear to be present in correspondence of the left tube, as shown by transverse investigations to the axis of the left tube from the right tube (sections identified by destructive drilling A-A), (figure 4).

ISSN 2319–7757 EISSN 2319–7765 I OPEN ACCESS

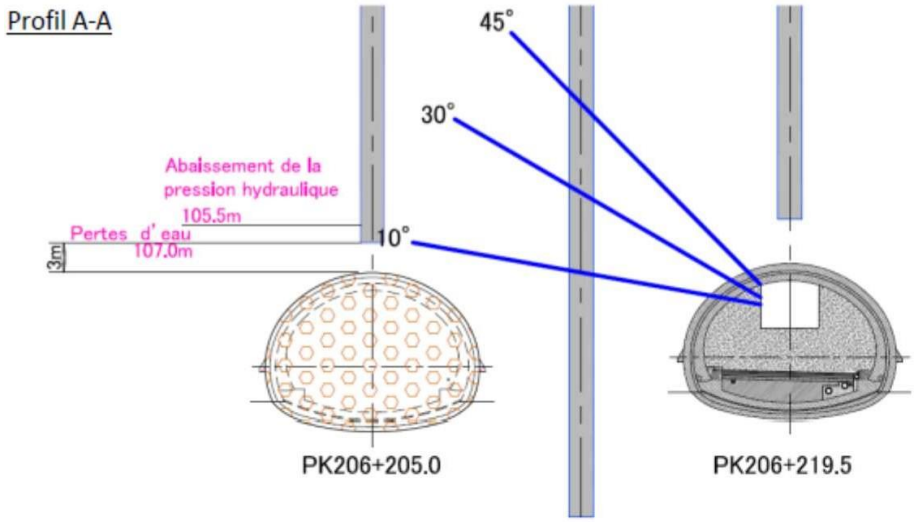

Figure 4 : Sections identified by destructive boreholes A-A.

The level of the curve along the left tube is shown by the red line in Figure (5). The samples boxes from V1, the only core, confirm this geometry and they do not show a decrease in the compactness of the soil surrounding the tunnel as a function of the depth. At the time of the partial landslide/ collapse, all the decompressed ground enters the tunnel and the curve forms; the height of the curve gives an appreciation of the level of decompression of the surrounding ground just before the landslide. It can be seen that the maximum height of the curve detected by the surveys is located in correspondence with the pedestrian passage gallery CP2.

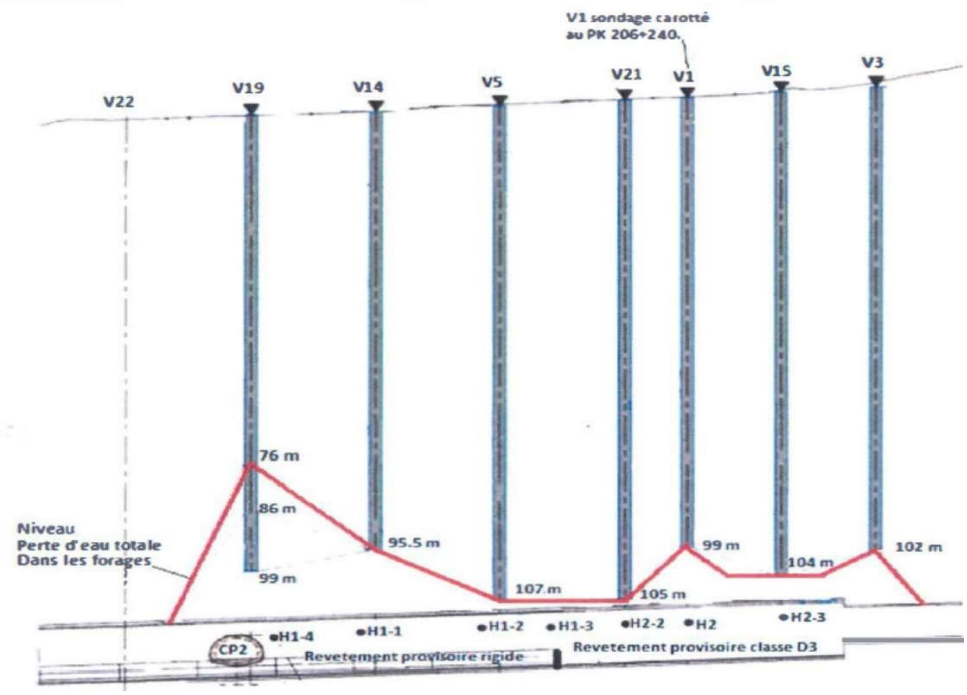

Figure 5 : Profile of the curve in axis to the left tube.

The samples obtained by the horizontal boreholes (H) carried out from the left tube to the right tube; clearly show that the landslide caused the collapse of the soil inside the excavation in the area between the plot 62 and plot 71. This phenomenon is confirmed by drillings from the southern tunnel forehead. Indeed, the 4 holes drilled forward (both at the axis of the tube and laterally) indicate that the colluvium is present up to 40 m beyond the working face/ tunnel forehead (approximately kp 206 + 150) and that the hangers have collapsed (the boreholes have intercepted parts of these supports in the center of the section up to 33m beyond the tunnel forehead (figure 6). In addition, the two inclined boreholes with a 30 ° slope have identified colluvium also above the tunnel key, in accordance with the diagram described in figure (5).

ISSN 2319–7757 EISSN 2319–7765 I OPEN ACCESS

(a) (b)

Figure 6. *a)* Conditions before the southern landslide front at plot 62, b) Photo of the northern landslide forehead from kp 206 + 330 (plot 71).

On the north side, the collapse of the left tube touches the pilot gallery at plot 71, with consequent heaving against the vault (figure 7). Note that during the digging of the investigation gallery at the southern forehead of the landslide, the left side of the left tube of hanger 844 (PK206 + 166, CP2) was found sheared in correspondence of the connection plate with the arched hanger contrary to what was recorded by the other 4 hangers (south side) which were subjected to fall.

Figure 7 : Preliminary investigation of 844th support at T1 south left.

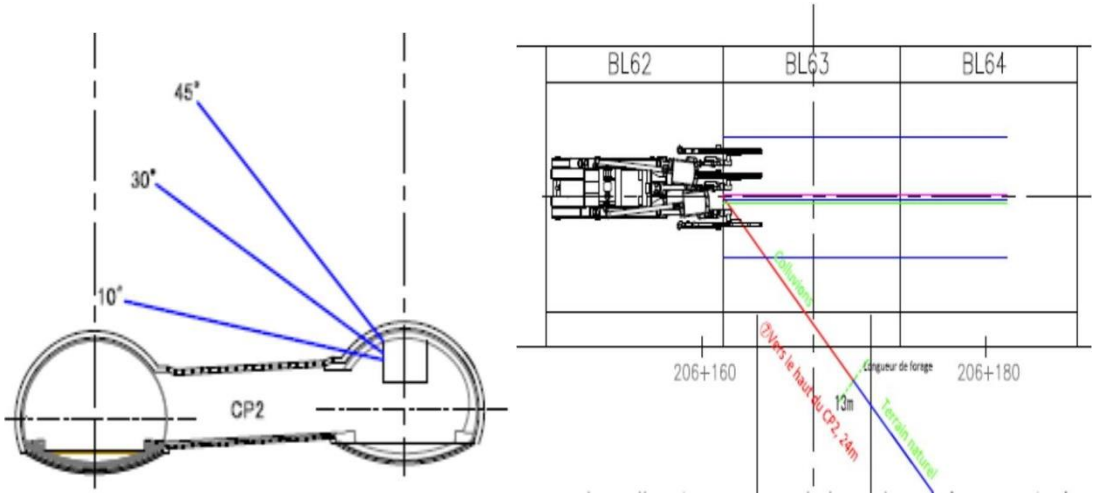

Figure 8 : Drilling carried out in correspondence with CP2.

ISSN 2319–7757 EISSN 2319–7765 I OPEN ACCESS

The landslide front has reached plot 61 on the left and CP2 is partly filled. The 4 holes drilled above the key of CP2 (1 from the southern landslide of the left tube and 3 from the right tube) confirm the good condition of the natural ground above the pedestrian gallery (figure 8).

The damage (destruction) shown by the photos and by the shotcrete deformation plan of the pilot gallery is summarized below;

- Detachment of the final coating concrete from the calotte and the sides of the tunnel for 20 m from the southern forehead of the landslide,
- Heaving of the invert seen from PK206 + 320 with a length of 35m towards the south.

Figure 9 : Photo of the current section of the straight tube.

After the collapse, the left tube was secured by making lean concrete infill between plot 63 and 72. Figure (9) shows the filling section, designed to allow accessibility of the tunnel in order to carry out future investigations and tunnel ground improvements.

4. CALCULATION MODEL AND REPAIR STUDY FOR THE T1 TUNNEL

The stability of deep tunnels made in half-sections has long been a major challenge for the scientific community. For about thirty years, new techniques, based on the installation of a pre-support system in front of tunnel forehead have been developed. They aim to control deformations and surface settlements induced by excavation and to ensure the stability of the structure in the long term [56]. The analysis of geotechnical projects is possible thanks to numerous finite element codes. In this work, we made a contribution to the numerical modeling of a tunnel T1 section reinforced by two pre-support systems; the bolting to the tunnel forehead and the umbrella vault. We will make an approximate model on the digging of a tunnel using PLAXIS 2D software which is based on the de-confinement of the soil, to facilitate the calculation the in situ measurements were taken into consideration to estimate the de-confinement of each calculation phase.

Plaxis 2D is a two-dimensional finite element code specially designed to perform deformation and stability analyzes for different types of geotechnical applications. Real situations can be represented by a plane or axisymmetric model. The code uses a convenient graphical interface allowing users to quickly generate a geometric model and a finite element mesh based on the vertical section of the structure to be studied. The Iraratna Model [1988, 1990] [52, 57] was used to determine the equivalent geotechnical characteristics of the structure to be repaired. During this study, the repair phasing of the old tube was taken into consideration phase by phase with an elastoplastic constitutive law. To facilitate the calculation, in situ measurements were implemented to estimate the de-confinement at each calculation phase. The Mohr-Coulomb elasto-plastic model was chosen for the simulation of our project, the advantage of this model lies in its simplicity. The section studied is presented in figures (10 and 11) of 200 m wide and 170 high.

ISSN 2319–7757 EISSN 2319–7765 I OPEN ACCESS

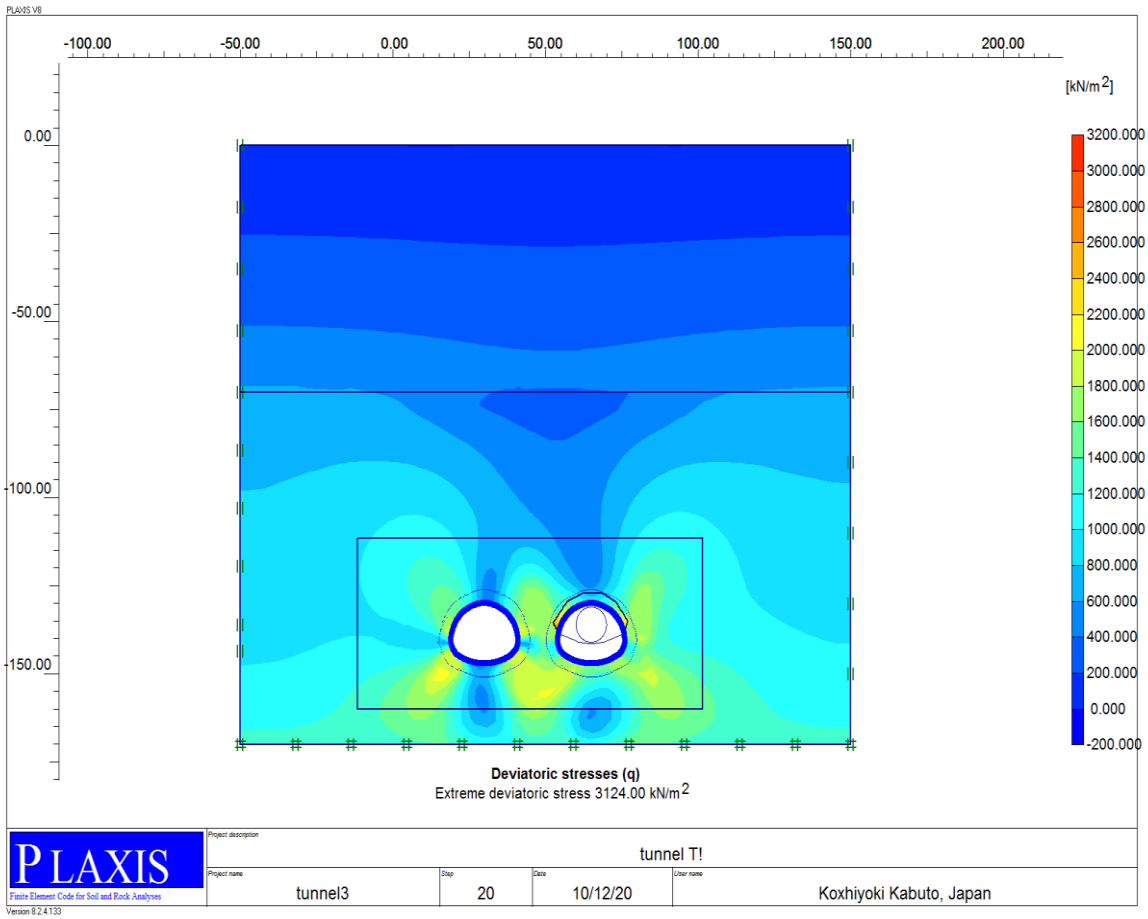

Figure 10: Scheme of the shear stresses evolution in the entire model.

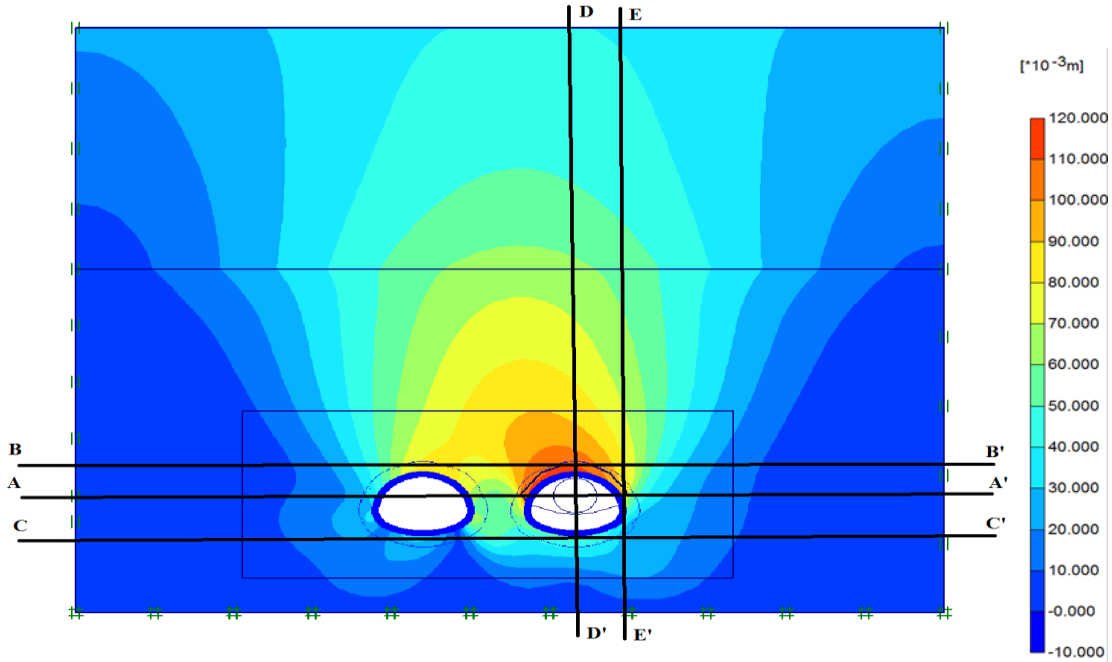

Figure 11 : Representative diagram analysis plans of the calculation result of the total displacements.

The characteristics of deformability and resistance of the rock mass used during the conceptual analysis phase are indicated in table (1), according to the geomechanical classification method "Rock Mass Rating (RMR)". Table (1) shows the

estimated RMR values for the Cretaceous Claystones on the basis of in situ and laboratory investigations available following the campaign carried out before the landslide. The geotechnical parameters of the claystones derive from the analysis of the results of the reconnaissance campaigns before and after the excavation; As well as the complementary recognition campaign.

Table 1 : The RMR classification and the geotechnical parameters of the T1 tunnel ground.

ID	Unit	0< Hz <70	Hz > 70
Material		Claystone/ Shale	Claystone/ Shale
RMR	**(U4)**	28	28
Rock Class		IV	IV
failure criterion		Mohr-Coulomb	Mohr-Coulomb
Volume weight γ	(kN/m^3)	24	24
Friction angle Φ	°	18	18
Cohesion C	(KPa)	25+2.5z	200
Young's modulus E	(MPa)	2818	2818
Poisson's ratio ν		0.3	0.3
Tensile strength σ	(KPa)	60	60

The materials used in this project comply with the operational needs imposed by Algerian (RPOA 2008 2), European (EC2, EC3) and international (model code) standards. Table (2) summarizes the different types of concrete used, the different types of steels used according to EC2 and EC3, the fiberglass used for the bolts and characteristics of the provisional support and final coating of the left tube and final coating right tube.

Table 2: Material characteristics.

Shotcrete (provisional support)		
Class		C30/37
Cylindrical characteristic resistance in compression	F_{ck}[MPa]	30
Design compressive strength Ultimate Limit State" ULS"	F_{cd}[MPa]	20
Deformation Modulus at 28 days	E_c[MPa]	29700
Poisson's ratio	V [-]	0.2
Steel for reinforced concrete		
Class		B500S
Tensile strength	F_{tk}[MPa]	600
Characteristic tension of elasticity	F_{yk}[MPa]	500
Design tensile strength Ultimate Limit State" ULS"	f_{yd}[MPa]	435
Deformation Modulus	E_s[MPa]	200000
Poisson's ratio	V [-]	0.3
Steel for hangers		
Class		S275
Tensile strength	F_{tk}[MPa]	430
Characteristic tension of elasticity	F_{yk}[MPa]	275
Design tensile strength Ultimate Limit State" ULS"	f_{yd}[MPa]	275
Deformation Modulus	E_s[MPa]	210000
Poisson's ratio	V [-]	0.3
Steel for pre-support pipe		
Class		S355
Tensile strength	F_{tk}[MPa]	500

ISSN 2319–7757 EISSN 2319–7765 I OPEN ACCESS

Characteristic tension of elasticity	F_{yk}[MPa]	355
Design tensile strength Ultimate Limit State" ULS"	f_{yd}[MPa]	355
Deformation Modulus	E_s[MPa]	210000
Poisson's ratio	V [-]	0.3
Fibre de verre		
Shear strength	T_{tk}[MPa]	150
Characteristic tension of elasticity	F_{yk}[MPa]	750
Design tensile strength Ultimate Limit State" ULS"	f_{yd}[MPa]	600
Deformation Modulus	E_s[MPa]	40000
Poisson's ratio	V [-]	0.2

Left Tube Characteristics				
	EA(kN/m)	**EI(kN.m²)**	**d(m)**	v
Provisional support	1.196 x10^7	1.272x10^5	0.357	0.2
Final coating	3.220 x10^7	3.549 x10^6	1.5	0.2
Right Tube Characteristics				
	EA(kN/m)	**EI(kN.m²)**	**d(m)**	v
Final coating	1.309 x10^7	1.632 x10^5	0.387	0.2

Calculation of reinforced geomechanical properties from the Iraratna Model [1988, 1990]

Indraratna & Kaiser [1988, 1990] performed axisymmetric calculations by simulating reinforced rock with improved geomechanical properties (C_{renf} et ϕ_{renf}). These characteristics are related to the bolting density by the coefficient;

$$\beta=\pi d\lambda a/Sh\ Sv \quad (1)$$

With :

d=60 mm : bolt diameter,

λ=1: coefficient of friction between bolt and rock,

a=9.58 m : tunnel radius,

S_h = 0.7 m

S_v : varies between 0.5 m and 1.2 m,

Takes it: Sv = 0.85 m.

S_h and S_v respectively represent the horizontal and vertical distance between the bolts and which are defined as follows.

$$\sin\phi renf = \frac{\beta(1+\sin\phi)+2\sin\phi}{\beta(1+\sin\phi)+2} \quad (2)$$

$$Crenf = \frac{2c\cos\phi\ (1-\sin\phi renf)(1+\beta)}{2\cos\phi renf\ (1-\sin\phi)} \quad (3)$$

Numerical application:

$$\beta=3.14\times(0.06)\times(9.58)\times 1/(0.7)\times(0.85) \quad (4)$$

➔ **β=3.033**

$$\sin\phi renf = \frac{3.033\times(1+\sin(18))+2\times\sin(18)}{3.033\times(1+\sin(18))} = 0.7685 \quad (5)$$

➔ $\boldsymbol{\phi renf = 50.22^o}$

$$Crenf = \frac{2\times200\times\cos(18)\times(1-\sin(50.22))\times(1+3.033)}{2\times\times\cos(50.22)\times(1-\sin(18))} \quad (6)$$

C_{renf} = 393.14 kPa

Takes it: **C_{renf} = 395 kPa**

ISSN 2319–7757 EISSN 2319–7765 I OPEN ACCESS

5. RESULTS AND DISCUSSIONS

5. 1. The Displacements:

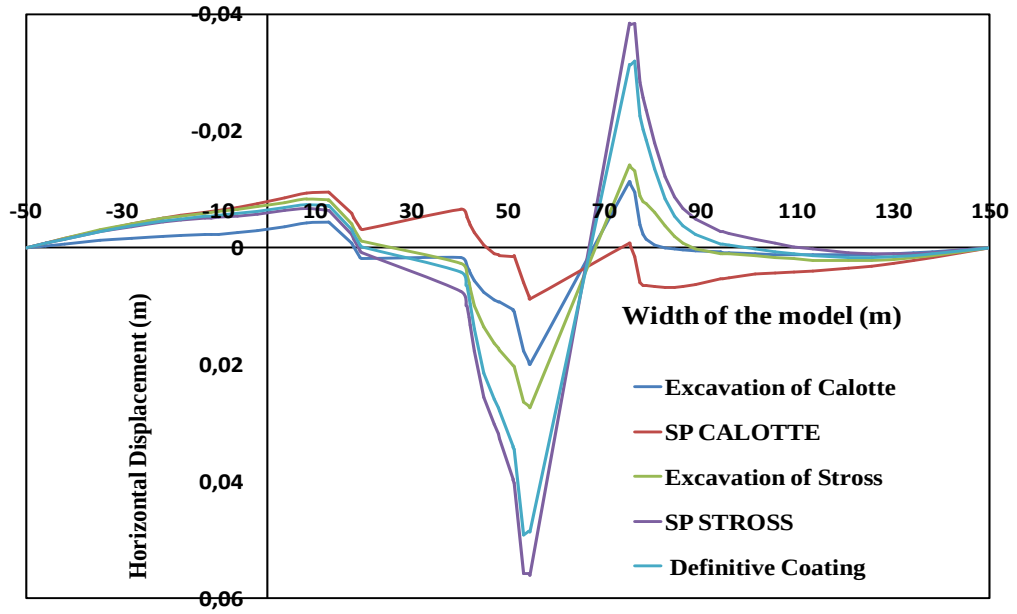

Figure 12. The variation of the horizontal displacement during the excavation phases (section Plan AA ').

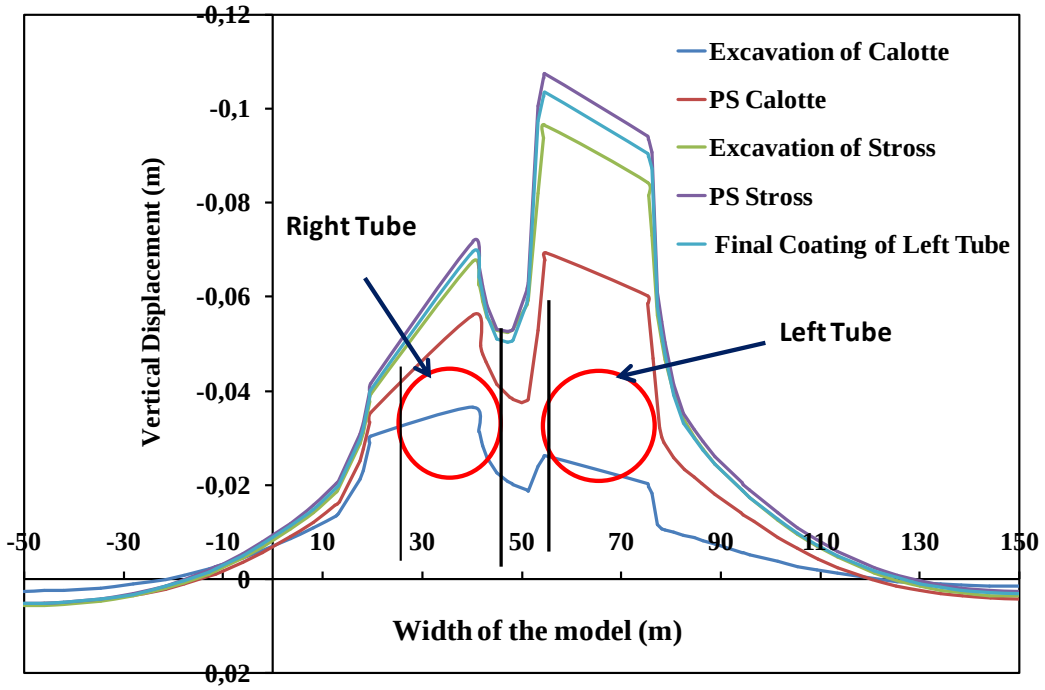

Figure 13. The vertical displacement variation according to the repair construction phases (Section Plan AA').

Figure (12) shows the variation of the horizontal displacement at the top of the arch (at the Calotte). The right tube is located between 19 m and 41m and the left tube is located between 54m and 76m, we notice that the displacement of the right tube is opposed to the displacement of the left tube and which does not exceed 1 cm, by against; the left tube reaches a maximum displacement for a value of 4 cm and at the left extremity the horizontal displacement is of the order of 5 cm. On the other hand, we note that the displacement values in the calotte excavation phase vary between -1 cm and 2 cm; and after the installation of

ISSN 2319–7757 EISSN 2319–7765 I OPEN ACCESS

provisional support the displacement is significantly reduced, but during the placement of the provisional support of the Stross (Bench), a considerable increase in displacement was marked between -3.8 cm and 5.5 cm, this is not the case of the excavation phase thereof, in which the displacement is varies between -1.4 cm and 2.7 cm and in the last one, which is the installation of the final coating, the horizontal displacement decreased compared to the displacement caused by the realization of the previous phase.

Figure (13) shows the variation of the vertical displacement during the phases of carrying out repair work on the destroyed tunnel (reinforcement phase), during excavation work the two tubes undergo differential settlements when passing from one tube to another and when passing from one phase to another. In the right tube the settlement is increased to a value of 7 cm at the right extremity, on the other hand in the left tube the settlement has been increased to 11 cm at the left extremity, by de-confinement effect of the left grounds.

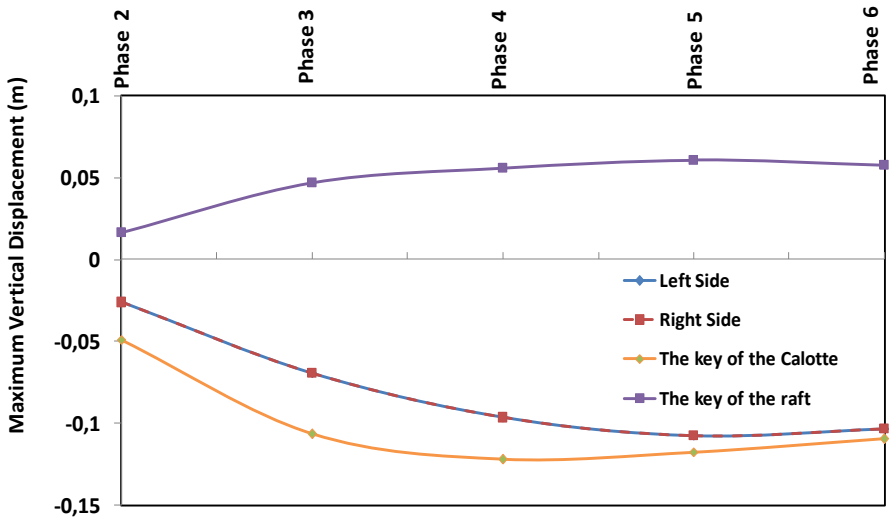

Figure 14. Maximal Vertical displacement at the tubes extremities (Section Plans BB′ and CC′).

Figure (14) shows that the increase in settlement at the points on both left and right sides is proportional to the rate of excavation progress, and at the level of the calotte key the settlement is much greater than those of the two extremities of the left tube, on the other hand the invert key marked an increase in heaving depending on the tunnel repair construction phases.

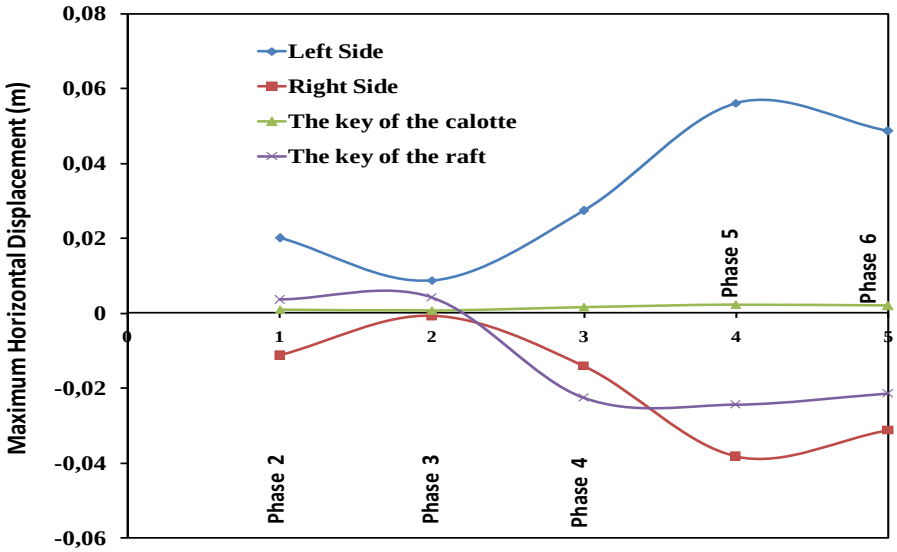

Figure 15. Maximum Horizontal displacement at the tubes extremities (Section Plans BB′ and CC′).

Figure (15) shows the evolution of the horizontal displacement at the two extremities of the left tube, the tunnel repair construction phases cause an earth pressure effect in both left and right sides, during the first two phases the earth pressure is

reduced on both sides; and after the Stross excavation and the placement of provisional support the earth pressure effect is increased to a maximum displacement value of 5.7 cm in the left side and 4 cm in the right side. After the completion of the final coating, the earth pressure is reduced to 5 cm on the left side and to 3 cm on the right side, but at the level of the calotte key and Stross the decrease in thrust is very remarkable.

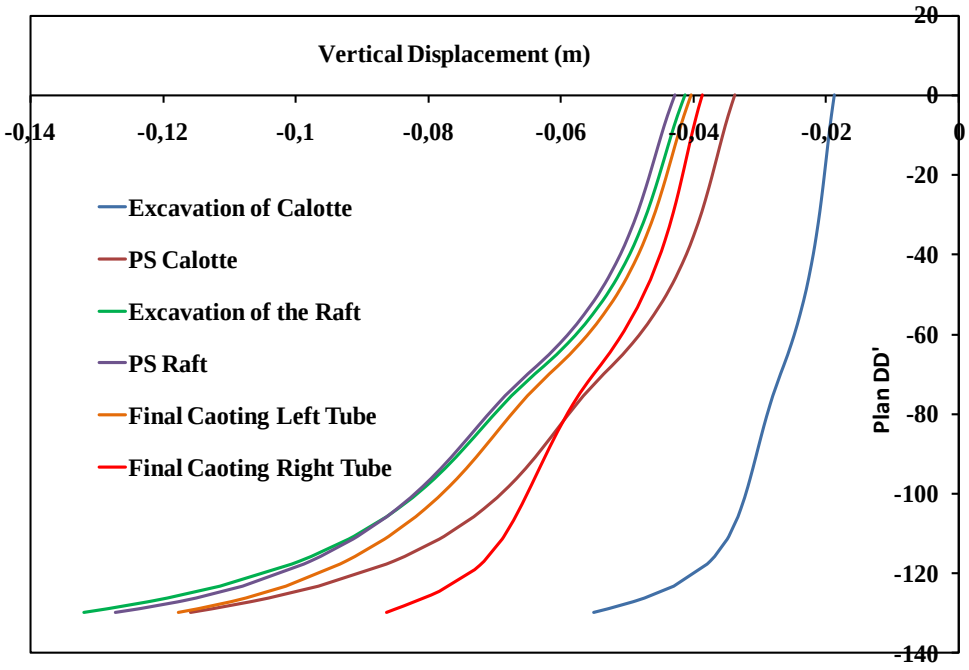

Figure 16. Vertical displacement at the calotte key (Section Plan DD').

After carrying out the excavation phases at the level of the left tube, we noticed that there is an increase in settlement that is proportional with the excavation progress rate but just after the installation of the final coating the settlement is remarkably reduced (figure 16). But at the right tube at the final coating sitting phase, the reduction in settlement is much greater than that of the left tube.

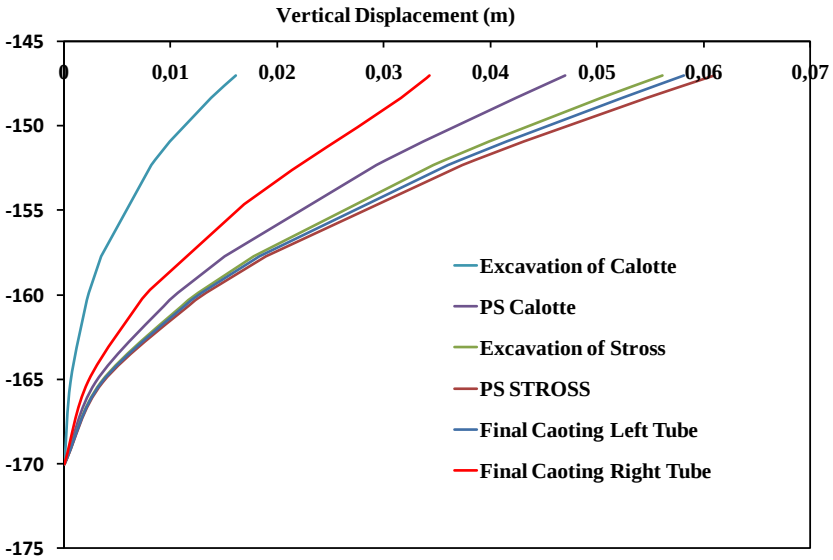

Figure 17. Vertical displacement at the invert key (Section Plan DD').

ISSN 2319–7757 EISSN 2319–7765 I OPEN ACCESS

The results presented in figure (17) show the vertical displacements variation according to the depth at the invert key, we notice that there is an increased heaving of 6.2 cm at the phase of the provisional support sitting of stross and in the last phase this heaving decreased to 5.9 cm in the left tube, on the other hand at the level of the right tube the heaving marked an offset of 2.5 cm.

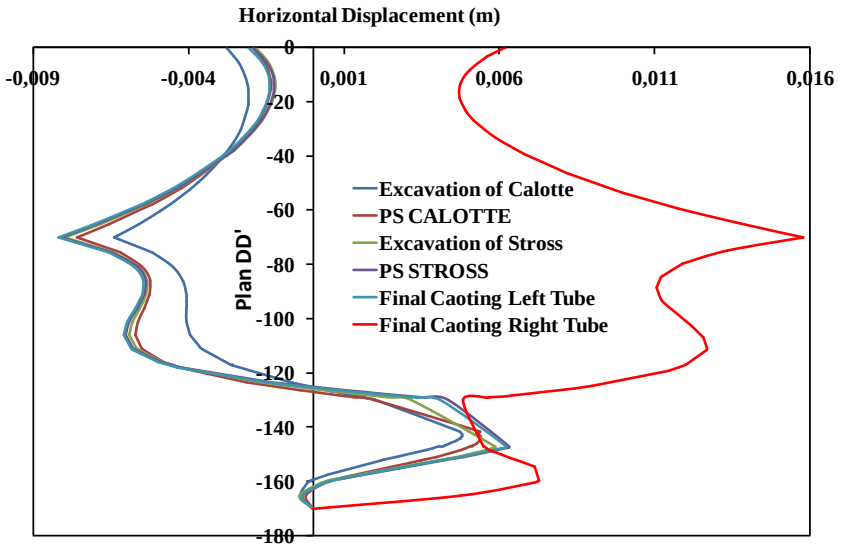

Figure 18. Horizontal displacement at the level of the Invert key and the Calotte Key (Section Plan DD')

Figure (18) represents the evolution of horizontal displacement with the left tube key (Stross and Calotte), in this modeling the excavation phases cause an active earth pressure effect on the left tube from 0 m up to 129 m and an passive earth pressure effect that starts from 145 m to the end of the profile. On the other hand, in the right tube there is only one effect which is the passive earth pressure over the entire depth because of the excavation phases completion on the left tube.

5.2. The Stresses:

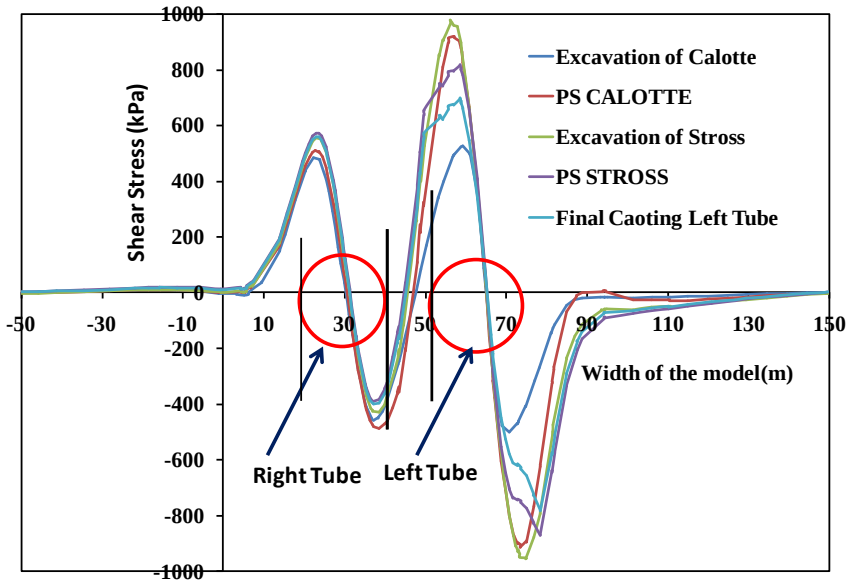

Figure 19. The variation of shear stress at Section Plan BB'.

Figure (19) represents the shear stress variation during the excavation phases execution, in the right tube the shear stress is varied between 600 kPa on the left side and -500 kPa on the right side with a imperceptible growth between the phases of the repair realization, but in the left tube we notice that the growth of the shear stress is very significant during the excavation phases in a maximum interval varies between 950 kPa in both sides.

ISSN 2319–7757 EISSN 2319–7765 I OPEN ACCESS

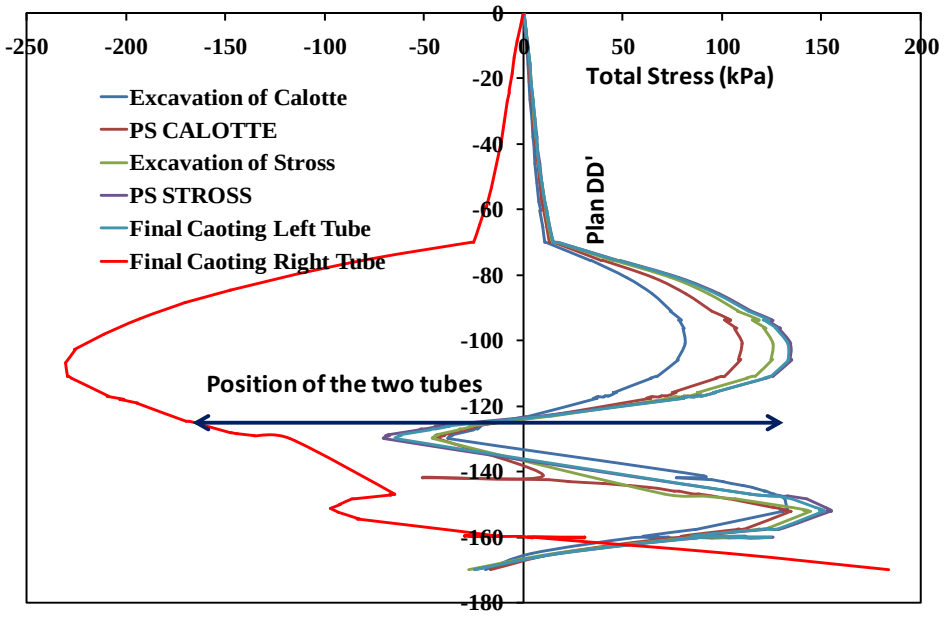

Figure 20. The variation of shear stress at Section Plan DD'.

In figure (20) the variation of the shear stress is presented, the maximum stress is located below the tunnel at a depth of 148 m with a positive value of 150 kPa but at the Calotte key the stress is negative for a value of 75 kPa in the phase of the provisional support sitting of the Bench (Stross). Above the left tube the stress is positive; on the other hand the stress in the right tube at the final phase has become negative, with a maximum value of 230 kPa.

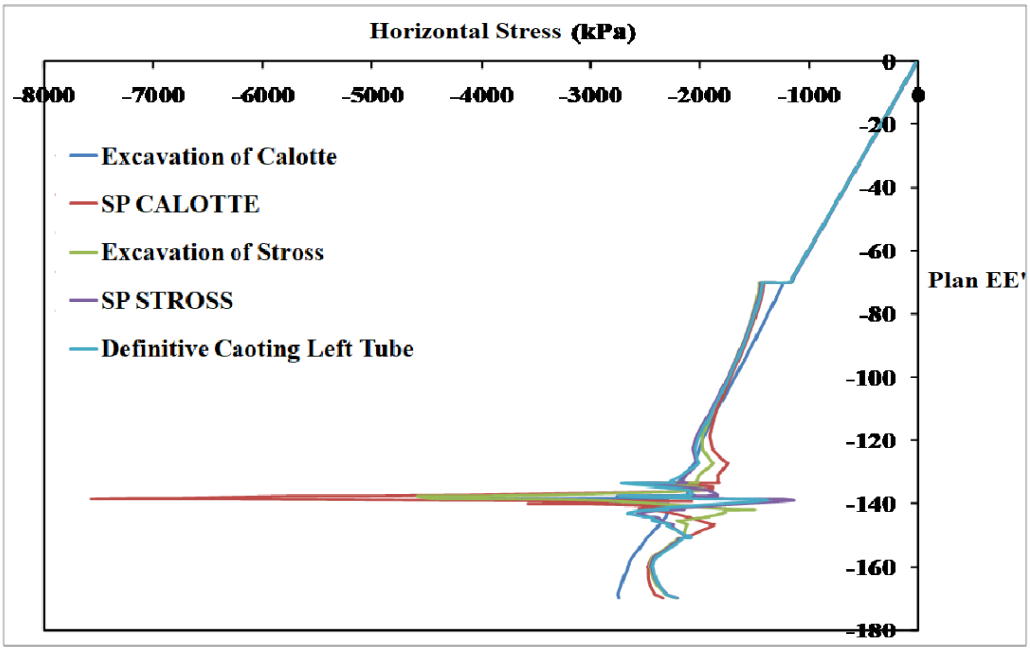

Figure 21. Evolution of the horizontal stress at Section Plan 'EE'.

Figure (21) shows that the increase in the horizontal stress is proportional to the increase in the depth of the tunnels, the maximum value of the earth pressure is 7500 kPa in the 2nd phase of the repair construction (SP Calotte/ Crwon) and will be reduced up to 2700 kPa in the last phase of the repair construction (the final coating location).

ISSN 2319–7757 EISSN 2319–7765 I OPEN ACCESS

6. CONCLUSION

The homogenization method was used for the determination of the numerical parameters of the 2D two-dimensional model, which represents the actual behavior of the tunnel during the repair phases of the old tunnel which was destroyed after commissioning, strengthening of the tunnel forehead by the fiberglass bolt method as well as the actual digging phasing were taken into consideration in the modeling. Thereby; the variation of vertical and horizontal displacements and the variation of the stresses are presented according to the tunnel repair realization phases on several plans.

On the basis of the results presented above, an interesting stability can be found in view of displacements and stress values of the repaired tunnel on several plans based on the Model of Iraratna [1988, 1990]. It is clear that strengthen the tunnel's forehead numerically and replaces the bolts and the ground / bolt interaction with an equivalent parameter (the increase in soil cohesion and friction angle) improves the value of the tunnel's displacements and stress. If the value of the cohesion and friction angle increases, the evolution of settlement decrease what involved the stability of tunnel's forehead.

Funding

This study has not received any external funding.

Conflict of Interest

The author declares that there are no conflicts of interests.

Data and materials availability

All data associated with this study are present in the paper.

REFERENCES AND NOTES

1. Houssam Khelalfa, June 2020. Tunnel Executors- NATM's Recommendations and Guidelines. LAMBERT Academic Publishing. ISBN: 978-620-2-67199-6.
2. Houssam Khelalfa, "Technical Analysis and Monitoring of Rock Mass Behavior During The Provisional Support Phase of The Texanna Twin-Tube Tunnel In Jijel Province, Algeria," International Journal of Advanced Engineering and Management, Vol. 4, No. 1, pp. 16-28, 2019
3. D. Wu, K. Xu, P. Guo, G. Lei, K. Cheng, and X. Gong, "Ground deformation characteristics induced by mechanized shield twin tunnelling along curved alignments," Advances in Civil Engineering, vol. 2021, Article ID 6640072, 17 pages, 2021. DOI: 10.1155/2021/6640072
4. Golser J, Mussger K. New Austrian Tunnelling Method (NATM), contractual aspects. In: Tunnelling under Difficult Conditions, Proceedings of the International Tunnel Symposium, Tokyo. Pergamon Press; 1979. p. 387–92.
5. Brown ET. Putting the NATM into perspective. Tunnels & Tunnelling International 1981; 13(10):7–13.
6. Aygar EB, Evaluation of new Austrian tunnelling method applied to Bolu tunnel's weak rocks, Journal of Rock Mechanics and Geotechnical Engineering, https://doi.org/10.1016/ j.jrmge.2019.12.011.
7. U.S. Army Corps of Engineers, "Engineering and Design Tunnels and Shafts in Rock (e-book)", Chapter 5, May 1997
8. OLOFSSON O. S., "Applied Explosives Technology For Construction and Mining", Sweden 1990, pp 131-159
9. Mair R.J., Taylor R.N. (1997): Bored tunnelling in the urban environment, Proceedings of the 14th International Conference on Soil Mechanics and Foundation Engineering, Balkema, Rotterdam, pp. 2353-2385.
10. Peck, R.B. (1969): Deep excavations and tunnelling in soft ground, State of the art report, in proceedings of the VII Int. Conf. on Soil Mechanics and Found. Eng., Mexico city, State of the art volume, pp. 225-290.
11. Manassero, Vittorio; Di Salvo, Giuseppe; Giannelli, Fabio; and Colombo, Giuseppe, "A Combination of Artificial Ground Freezing and Grouting for the Excavation of a Large Size Tunnel Below Groundwater" (2008). International Conference on Case Histories in Geotechnical Engineering. 2.
12. Harris, J.S. [1995]. "Ground freezing in practice". Thomas Telford
13. Petr Nikolaev, Mikhail Shuplik, January 2019, Low-temperature ground freezing methods for underground construction in urban areas. MATEC Web of Conferences 265:04020. DOI: 10.1051/matecconf/201926504020
14. Dingli Zhangn, Qian Fang and Haicheng Lou. Grouting techniques for the unfavorable geological conditions of Xiang'an subsea tunnel in China. Journal of Rock Mechanics and Geotechnical Engineering. Volume 6, Issue 5, October 2014, Pages 438-446. DOI: 10.1016/j.jrmge.2014.07.005
15. Tornaghi, R., B Bosco and B. De Paoli. 1988. "Application of recently developed grouting procedures for tunnelling in

the Milan urban area". Fifth International Symposium on Tunnelling – April 18-21. London.
16. Sopacı, E., & Akgün, H. (2008). Engineering geological investigations and the preliminary support design for the proposed Ordu Peripheral Highway Tunnel, Ordu, Turkey. Engineering Geology, 96(1-2), 43-61.
17. G. W. Clough, B. P. Sweeney, and R. J. Finno, "Measured soil response to EPB shield tunneling," Journal of Geotechnical Engineering, vol. 109, no. 2, pp. 131–149, 1983.
18. Anagnostou G, Kovári K (1994) The face stability of slurry shield-driven tunnels. Tunneling and Underground Space Technology 9(2):165-174, DOI: 10.1016/0886-7798(94)90028-0
19. Broere W, van Tol AF (2000) Influence of infiltration and groundwater flow on tunnel face stability. In: Kusakabe O, Fujita K, Miyazaki Y (eds) Geotechnical aspects of underground construction in soft ground. Balkema, Rotterdam, 339-344
20. Lee CJ, Wu BR, Chen HT, Chiang KH (2006) Tunneling stability and arching effects during tunneling in soft clayey soil. Tunnelling and Underground Space Technology 21(2):119-132, DOI: 10.1016/j.tust.2005.06.003
21. Hoek, E., Kaiser, P. K., & Bawden, W. F. (2000). Support of underground excavations in hard rock. CRC Press
22. Schubert W. Basics and Application of the Austrian Guideline for the Geomechanical Design of Underground Structures. In: EUROCK 2004 & 53rd Geomechanics Colloquium; 2004.
23. Wang X, Lai J, Garnes RS, Lou J. Support system for tunnelling in squeezing ground of Qingling-Daba mountainous area: A case study from soft rock tunnels. Advances in Civil Engineering 2019. https://doi.org/10.1155/2019/8682535.
24. R. J. Finno and G. W. Clough, "Evaluation of soil response to EPB shield tunneling," Journal of Geotechnical Engineering, vol. 111, no. 2, pp. 155–173, 1985.
25. Zhen Liu, Cuiying Zhou, Yiqi Lu, Xu Yang, Yanhao Liang and Lihai Zhang. Application of FRP Bolts in Monitoring the Internal Force of the Rocks Surrounding a Mine-Shield Tunnel. Sensors 2018, 18(9), 2763; https://doi.org/10.3390/s18092763
26. Nikolaev, N. 1989. Development of the theory and practice of rock bolting in underground excavations. Dissertation. Sofia, UMG.
27. Li CC, Principles of rockbolting design, Journal of Rock Mechanics and Geotechnical Engineering (2017), doi: 10.1016/j.jrmge.2017.04.002.
28. Aksoy CO, Onargan T. The role of umbrella arch and face bolt as deformation preventing support system in preventing building damages. Tunnelling and Underground Space Technology 2010; 25(5): 553-9.
29. Lang TA. Theory and practice of rockbolting. Transactions of American Institute of Mining, Metallurgical, and Petroleum Engineers 1961; 220: 333-48.
30. Nomikos PP, Sofianos AI, Tsoutrelis CE. Symmetric wedge in the roof of a tunnel excavated in an inclined stress field. International Journal of Rock Mechanics and Mining Sciences 2002; 39(1): 59-67.
31. Panek LA. Design for bolting stratified roof. Transactions of the Society of Mining Engineers 1964; 229: 113-9.
32. Stillborg B. Professional users handbook for rockbolting. Trans Tech Publications. Clausthal-Zellerfeld, 1994.
33. Charlie C. Li. Principles of rockbolting design. Journal of Rock Mechanics and Geotechnical Engineering. Volume 9, Issue 3, June 2017, Pages 396-414. https://doi.org/10.1016/j.jrmge.2017.04.002
34. V. Marinos, A. Goricki, and E. Malandrakis, "Determining the principles of tunnel support based on the engineering geological behaviour types: example of a tunnel in tectonically disturbed heterogeneous rock in Serbia," Bulletin of Engineering Geology and the Environment, vol. 78, no. 4, pp. 2887–2902, 2019.
35. Nomikos PP, Yiouta-Mitra PV, Sofianos AI. Stability of asymmetric roof wedge under non-symmetric loading. Rock Mechanics and Rock Engineering 2006; 39(2): 121-9.
36. Ocak I. Control of surface settlements with umbrella arch method in second stage excavations of Istanbul Metro. Tunnelling and Underground Space Technology 2008; 23(6): 674-81.
37. Volkmann GM, Schubert W. Effects of pipe umbrella systems on the stability of the working area in weak ground tunneling. In: Sinorock - International Symposium on Rock Characterisation, Modelling and Engineering Design Methods. International Society for Rock Mechanics; 2009.
38. Ruwan Rajapakse PE, CCM, CCE, AVS. November 2015.Tunnel design. Geotechnical Engineering Calculations and Rules of Thumb (Second Edition).2016, Pages 337-345. DOI: 10.1016/B978-0-12-804698-2.00035-0
39. Burland, J.B., 1995. Assessment of risk of damage to buildings due to tunnelling and excavation. Proc. 1st Int. Conf. on Earthquake Geot. Eng., IS-Tokyo, pp. 611 – 628.
40. Jing, L. (2003). A review of techniques, advances and outstanding issues in numerical modelling for rock mechanics and rock engineering. International Journal of Rock Mechanics and Mining Sciences, 40(3), 283-353.
41. Gurocak, Z., Solanki, P., & Zaman, M. M. (2007). Empirical and numerical analyses of support requirements for a diversion tunnel at the Boztepe dam site, eastern Turkey. Engineering geology, 91(2-4), 194-208.
42. Bobet, A. (2010). Numerical methods in geomechanics. The Arabian Journal for Science and Engineering, 35(1B), 27-48.

ISSN 2319–7757 EISSN 2319–7765 | OPEN ACCESS

43. Asef, M. R., Redddish, D. J., Lloyd, P.W. (2000). Rock–support interaction analysis based on numerical modeling. Geotechnical and Geological Engineering 18: 23–37
44. Thomas Kasper and Günther Meschke. December 2004. A 3D finite element simulation model for TBM tunnelling in soft ground. International Journal for Numerical and Analytical Methods in Geomechanics 28(14):1441 - 1460. DOI: 10.1002/nag.395
45. A. Lambrughi, L. Medina Rodríguez, and Riccardo Castellanza.March 2012. Development and validation of a 3D numerical model for TBM–EPB mechanised excavations. Computers and Geotechnics 40:97–113. DOI: 10.1016/j.compgeo.2011.10.004
46. Maciej Ochmański. May 2015. Numerical model for slurry shield TBM tunnelling. Conference: XV Scientific Conference for Civil Engineering At: Szczyrk, Poland.
47. Michael Kavvadas. June 2005. Monitoring ground deformation in tunnelling: Current practice in transportation tunnels. Engineering Geology 79(1):93-113. DOI: 10.1016/j.enggeo.2004.10.011
48. Bock, H., 2001. European practice in geotechnical instrumentation for tunnel construction control. Tunnels and Tunnelling International, 51 – 54.
49. Sakurai, S. (1983). ''Displacement measurements associated with the design of underground openings.'' Proc., Int. Symp. Field Measurements in Geomechanics, Zurich, 2, 1163–1178.
50. V. Kontogianni and Stathis Stiros. June 2005. Induced deformation during tunnel excavation: Evidence from geodetic monitoring. Engineering Geology 79(1):115-126. DOI: 10.1016/j.enggeo.2004.10.012
51. Strauss A, Bien J, Neuner H, et al. Sensing and monitoring in tunnels testing and monitoring methods for the assessment of tunnels. Structural Concrete. 2020;21:1356–1376.https://doi.org/10.1002/suco.201900444.
52. Indraratna B, Kaiser PK (1990) Design for grouted rock boltsbased on the convergence control method. Int J Rock Mech Min Sci Geomech Abstr 27:269–281. DOI: 10.1016/0148-9062(90)90529-B
53. L Joleaud; M Ferrand; E Ficheur; Algeria. S Carte géologique de l'Algérie 1:50,000. 74, El Aria. ervice de la carte géologique de l'Algérie., 1908.
54. Chadi, M. (2004). Cadre géologique et structural des séries néritiques crétacées du constantinois. (Algérie Orientale). (Thèse d'Etat, Univ. Mentouri, Constantine, 2004).
55. Coiffait, Ph-E. (1992). Un bassin post-nappes dans son cadre structural: l'exemple du bassin de Constantine (Algérie nord-orientale). (Thèse Sciences, Univ. Nancy, 1992)
56. Zhao, YM., Feng, XT., Jiang, Q. et al. Large Deformation Control of Deep Roadways in Fractured Hard Rock Based on Cracking-Restraint Method. Rock Mech Rock Eng (2021). https://doi.org/10.1007/s00603-021-02384-4
57. B. Indraratna and P. K. Kaiser, "Analytical model for the design of grouted rock bolts," International Journal for Numerical and Analytical Methods in Geomechanics, vol. 14, no. 4, pp. 227–251, 1990. DOI: 10.1002/nag.1610140402

ISSN 2319–7757 EISSN 2319–7765 I OPEN ACCESS